

Contribution from Union Carbide Corporation, Tarrytown, New York 10591,
and the Department of the Geophysical Sciences, The University of Chicago, Chicago, Illinois 60637

Crystal Structure of $\text{AlPO}_4\text{-21}$, a Framework Aluminophosphate Containing Tetrahedral Phosphorus and both Tetrahedral and Trigonal-Bipyramidal Aluminum in 3-, 4-, 5-, and 8-Rings

J. MICHAEL BENNETT,[†] JANET M. COHEN,[†] GILBERTO ARTIOLI,[‡] JOSEPH J. PLUTH,[†]
and JOSEPH V. SMITH*[†]

Received May 29, 1984

The 21st member of a new group of synthetic aluminophosphates contains $4\text{Al}_3\text{P}_3\text{O}_{12}\text{OH}\cdot 1.33\text{N}_2\text{C}_7\text{H}_{21}$ in a monoclinic cell ($a = 10.3307$ (10), $b = 17.5241$ (13), $c = 8.6757$ (10) Å; $\beta = 123.369$ (7)°; $P2_1/a$). The aluminophosphate framework contains three types of tetrahedral P, two types of trigonal-bipyramidal Al, and one type of tetrahedral Al. A 3-ring is composed of two Al^{IV} atoms and one P^{IV} atom. Two types of 5-rings each contain two P^{IV} and two Al^{V} atoms and either another Al^{IV} or an Al^{V} atom, respectively. Edge-sharing 3- and 5-rings form an infinite chain. There are four types of 4-rings with alternating Al and P atoms, and two of the 4-rings generate an extended double-crankshaft chain. The 3D framework can be obtained by adding an up or a down branch to each node of a tessellation composed of 3-, 4-, 5-, and 8-rings. Pairs of adjacent Al^{V} atoms share a hydroxyl group whose mathematical removal yields a new 3D net containing 4-, 6-, and 8-rings. All oxygen atoms are linked to one Al and one P, and all interatomic distances in the framework are consistent with simple models involving near neighbors. The closer approach of three oxygens in the waist of the trigonal bipyramid to Al than for the two apical oxygens is explained by sp^2 hybridization. Hydrogen bonding across a 5-ring is probably important for structural stability. The N,N,N,N' -tetramethyl-1,3-propanediamine (TMPD) molecule used as an attempted template during synthesis split into three triatomic species, which were encapsulated by the aluminophosphate framework. The postulated trio of two dimethylammonium and one propyl species occupy different positions, and the overlap of electron density precludes unique identification.

A novel class of crystalline, microporous aluminophosphate phases^{1,2} represents the first group of molecular sieves with framework oxide compositions devoid of silica. Structural analogues of the zeolites sodalite and erionite were reported,^{1,2} and a novel structure was found for $\text{AlPO}_4\text{-5}$.^{2,3} These three structures contain 4-connected frameworks with both Al and P in tetrahedral coordination with oxygen. In natural compounds, aluminum can occur with 4-, 5-, and 6-coordination to oxygen, and the linkage of 5- and 6-coordinated Al to 4-coordinated Al and P in frameworks is certainly of theoretical interest, and possibly of practical value. The 15th member of the aluminophosphate group contains a complex framework composed of edge-sharing dimers of $\text{AlO}_4(\text{OH})_2$ octahedral linked through vertices to $\text{AlO}_4(\text{H}_2\text{O})(\text{OH})$ octahedra and PO_4 tetrahedra;⁴ small pores contain a hydrogen-bonded NH_4 ion and one water molecule. The latter can be removed apparently without collapse of the framework. We now report the crystal structure and unique framework of the 21st member of the aluminophosphate group. Whereas all the phosphorus is in tetrahedral coordination, the aluminum is split one-third into tetrahedral and two-thirds into trigonal-bipyramidal (fivefold) coordination. Furthermore, the vertex-shared framework contains three-, four-, five-, and eight-membered rings. Small cavities contain fragments of an organic molecule which was used as a trial template during synthesis.

Experimental Section

Monoclinic tablets flattened on (010) were synthesized from an aqueous mixture of phosphoric acid, pseudoboehmite alumina, and TMPD ($\text{N}_2\text{C}_7\text{H}_{18}$) held at 200 °C for 7 days. Sample 5599-85D consists mainly of pseudohexagonal tablets up to $70 \times 50 \times 20 \mu\text{m}$, many of which show simple twinning. The bulk analysis (34.0 wt % Al_2O_3 , 48.4 wt % P_2O_5 , 6.3 wt % C, 2.1 wt % N, 16.3 wt % loss on ignition) corresponds to the following number of atoms in the unit cell normalized to 24 (Al + P): Al, 11.9; P, 12.1; C, 9.3; N, 2.7. Interpretation of the loss on ignition is not certain because of lack of knowledge of the constituents. On the basis of the crystal structure data (see later), the unit-cell contents appear to be $4\text{Al}_3\text{P}_3\text{O}_{12}\text{OH}\cdot 1.33\text{N}_2\text{C}_7\text{H}_{21}$, for which 4 H^+ are added to the organic unit to balance the charge of the inorganic one.

The crystal structure was determined by using a standard phase-seeking procedure⁵ on an untwinned crystal $60 \times 40 \times 20 \mu\text{m}$ and refined with independent data on an untwinned crystal $100 \times 70 \times 40 \mu\text{m}$ (Table I⁶). Although the intensity data from the two crystals are consistent with space group $P2_1/a$, the high-angle diffractions on Weissenberg photographs with Cu $K\alpha$ radiation are doubled. The displacements did not

Table I. Crystallographic Experimental Conditions for $\text{AlPO}_4\text{-21}$ at Room Temperature

formula	$\text{Al}_3\text{P}_3\text{O}_{12}\text{OH}\cdot 1.33\text{N}_2\text{C}_7\text{H}_{21}$
fw	462.50
space group	$P2_1/a$
a	10.3307 (10) Å
b	17.5241 (13) Å
c	8.6757 (10) Å
β	123.369 (7)°
V, Z	1311.7 Å ³ , 4
calcd density	2.60 g/cm ³
no. of reflns for cell refinement	20 ($52^\circ < 2\theta < 72^\circ$)
cryst shape, size	(010) plate, $40 \times 70 \times 100 \mu\text{m}$
radiation (graphite monochromator), λ	Cu $K\alpha$, 1.5418 Å
diffractometer	Picker-KRISEL
range of hkl	$h, \pm k, \pm l$
scan technique, speed, bkgd	θ - 2θ , 2°/min, fixed 20 s
$(\sin \theta)/\lambda$ max	0.51 Å ⁻¹
no. of measd intensities	4810
no. of unique intensities	2184 (2007 > 2σ used in refinement)
max variation in std intensity	2.3%
abs coeff (abs)	67.0 cm ⁻¹ ($0.61 < \text{abs} < 0.78$)
refinement	$F; w = 1/\sigma^2(F)$
R, R_w, S	0.046, 0.042, 1.8
scattering factors f', f''	neutral
computer programs	SHELX76, ORTEP, ORFFE
max shift/esd, final cycle LS	0.101
min, max on final diff Fourier	-0.78, +0.99 e/Å ³

fit any obvious twin law and appear to result from two components with slightly different cell dimensions in parallel orientation. Structure refinement was straightforward for the atomic sites assigned to a framework (P(1)-P(3); Al(1)-Al(3); O(1)-O(13)) but was inconclusive for the

- (1) Wilson, S. T.; Lok, B. M.; Messina, C. A.; Cannan, T. R.; Flanigen, E. M. *J. Am. Chem. Soc.* **1982**, *104*, 1146-1167.
- (2) Wilson, S. T.; Lok, B. M.; Messina, C. A.; Cannan, T. R.; Flanigen, E. M. *ACS Symp. Ser.* **1983**, *No. 218*, 79-106.
- (3) Bennett, J. M.; Cohen, J. P.; Flanigen, E. M.; Pluth, J. J.; Smith, J. V. *ACS Symp. Ser.* **1983**, *No. 218*, 109-118.
- (4) Pluth, J. J.; Smith, J. V.; Bennett, J. M.; Cohen, J. P. *Acta Crystallogr., Sect. C*, in press.
- (5) Main, P.; Hull, S. E.; Lessinger, L.; Germain, G.; Delereq, J.-P.; Woolfson, M. M. "MULTRAN78" (a system of computer programs for the automatic solution of crystal structures from X-ray diffraction data); University of York: York, England, 1978.
- (6) Computer programs are listed in: Pluth, J. J.; Smith, J. V. *J. Am. Chem. Soc.* **1982**, *104*, 6977-6982.

[†] Union Carbide Corp.

[‡] The University of Chicago.

Table II. Atomic Positions and Root-Mean-Square Displacement for AlPO₄-21

	x	y	z	$u_{\text{eq}}^{1/2} \text{ \AA}$
P(1)	0.1335 (1)	0.0708 (1)	0.9738 (2)	0.086 (3)
P(2)	0.0269 (1)	0.2112 (1)	0.3235 (2)	0.094 (3)
P(3)	0.4967 (1)	0.1646 (1)	0.7462 (2)	0.091 (3)
Al(1)	0.3082 (1)	0.1714 (1)	0.3192 (2)	0.098 (3)
Al(2)	0.3372 (1)	0.3892 (1)	0.9739 (2)	0.088 (3)
Al(3)	0.2057 (1)	0.2037 (1)	0.7707 (2)	0.089 (3)
O(1)	0.3375 (3)	0.4885 (2)	0.0519 (4)	0.103 (7)
O(2)	0.2331 (4)	0.0912 (2)	0.1807 (4)	0.121 (6)
O(3)	0.4210 (4)	0.2188 (2)	0.2580 (4)	0.119 (6)
O(4)	0.0904 (4)	0.1947 (2)	0.5237 (4)	0.128 (6)
O(5)	0.0484 (3)	0.2523 (2)	0.7775 (4)	0.109 (6)
O(6)	0.4254 (4)	0.1411 (2)	0.5439 (4)	0.136 (6)
O(7)	0.4636 (3)	0.4153 (2)	0.9012 (4)	0.104 (7)
O(8)	0.1819 (3)	0.1203 (2)	0.8696 (4)	0.117 (6)
O(9)	0.3221 (4)	0.2905 (2)	0.8647 (5)	0.117 (6)
O(10)	0.3759 (3)	0.1525 (2)	0.7924 (4)	0.113 (6)
O(11)	0.1316 (3)	0.3898 (2)	0.8632 (4)	0.112 (6)
O(12)	0.1589 (4)	0.2283 (2)	0.2955 (5)	0.130 (6)
O(13)	0.4353 (4)	0.3575 (2)	0.2081 (4)	0.119 (6)
N(1)	0.2155 (9)	0.4898 (4)	0.2852 (11)	0.197 (8)
C(1)	0.3305 (13)	0.4857 (5)	0.4786 (16)	0.401 (7)
C(2)	0.0868 (9)	0.4358 (4)	0.2039 (11)	0.306 (6)
C(3)	0.177 (2)	0.4828 (9)	0.362 (3)	0.00 (7)
C(4)	0.125 (3)	0.4639 (12)	0.477 (3)	0.30 (2)
H(1)	0.381 (6)	0.286 (3)	0.854 (8)	0.16 (6)

^a $u_{\text{eq}}^{1/2}$ is the root-mean square-displacement (Å) for isotropic approximation.

contents of the channels. Five peaks were distinctly above background error, and the combined electron density was consistent with the 1.33 TMPD indicated by the bulk chemical analysis. However, it was not

Table III. Interatomic Distances (Å) and Angles (deg) in AlPO₄-21

P(1)-O(1)	1.514 (3)	P(2)-O(3)	1.530 (3)	P(3)-O(5)	1.524 (3)
P(1)-O(2)	1.542 (3)	P(2)-O(4)	1.509 (4)	P(3)-O(6)	1.540 (4)
P(1)-O(7)	1.524 (4)	P(2)-O(12)	1.540 (5)	P(3)-O(10)	1.521 (5)
P(1)-O(8)	1.522 (4)	P(2)-O(13)	1.518 (3)	P(3)-O(11)	1.525 (3)
av	1.526	av	1.524	av	1.528
Al(1)-O(2)	1.730 (3)	Al(2)-O(1)	1.867 (3)	Al(3)-O(4)	1.796 (3)
Al(1)-O(3)	1.736 (5)	Al(2)-O(7)	1.794 (5)	Al(3)-O(5)	1.864 (4)
Al(1)-O(6)	1.718 (3)	Al(2)-O(9)	1.936 (4)	Al(3)-O(8)	1.779 (4)
Al(1)-O(12)	1.751 (4)	Al(2)-O(11)	1.787 (3)	Al(3)-O(9)	1.830 (3)
av	1.734	Al(2)-O(13)	1.788 (4)	Al(3)-O(10)	1.889 (4)
		av	1.834	av	1.832
O(1)-P(1)-O(2)	109.5 (2)	O(3)-P(2)-O(4)	110.5 (2)	O(5)-P(3)-O(6)	111.1 (2)
O(1)-P(1)-O(7)	111.6 (2)	O(3)-P(2)-O(12)	107.4 (2)	O(5)-P(3)-O(10)	110.1 (2)
O(1)-P(1)-O(8)	107.5 (2)	O(3)-P(2)-O(13)	109.4 (2)	O(5)-P(3)-O(11)	112.1 (2)
O(2)-P(1)-O(7)	108.9 (2)	O(4)-P(2)-O(12)	110.9 (2)	O(6)-P(3)-O(10)	108.5 (2)
O(2)-P(1)-O(8)	109.4 (2)	O(4)-P(2)-O(13)	109.0 (2)	O(6)-P(3)-O(11)	106.3 (2)
O(7)-P(1)-O(8)	110.0 (2)	O(12)-P(2)-O(13)	109.6 (2)	O(10)-P(3)-O(11)	108.7 (2)
O(2)-Al(1)-O(3)	107.2 (2)	O(1)-Al(2)-O(7)	91.9 (2)	O(4)-Al(3)-O(5)	93.4 (2)
O(2)-Al(1)-O(6)	107.7 (2)	O(1)-Al(2)-O(9)	173.5 (2)	O(4)-Al(3)-O(8)	109.1 (2)
O(2)-Al(1)-O(12)	110.6 (2)	O(1)-Al(2)-O(11)	87.3 (2)	O(4)-Al(3)-O(9)	116.5 (2)
O(3)-Al(1)-O(6)	108.8 (2)	O(1)-Al(2)-O(13)	89.4 (2)	O(4)-Al(3)-O(10)	92.7 (2)
O(3)-Al(1)-O(12)	112.8 (2)	O(7)-Al(2)-O(9)	86.3 (2)	O(5)-Al(3)-O(8)	90.3 (2)
O(6)-Al(1)-O(12)	109.5 (2)	O(7)-Al(2)-O(11)	133.6 (2)	O(5)-Al(3)-O(9)	88.7 (2)
		O(7)-Al(2)-O(13)	114.3 (2)	O(5)-Al(3)-O(10)	173.6 (2)
		O(9)-Al(2)-O(11)	89.5 (2)	O(8)-Al(3)-O(9)	134.4 (2)
		O(9)-Al(2)-O(13)	97.0 (2)	O(8)-Al(3)-O(10)	86.0 (2)
		O(11)-Al(2)-O(13)	112.1 (2)	O(9)-Al(3)-O(10)	90.1 (2)
P(1)-O(1)-Al(2)	142.7 (3)	N(1)-C(1)	1.428 (13)	C(1)-N(1)-C(2)	118.9 (9)
P(1)-O(2)-Al(1)	139.0 (2)	N(1)-C(2)	1.458 (11)	C(1)-N(1)-O(1)	114.7 (8)
P(2)-O(3)-Al(1)	137.2 (3)	N(1)-C(3)	0.96 (3)	C(1)-N(1)-O(10)	105.7 (5)
P(2)-O(4)-Al(3)	160.0 (2)	N(1)-O(1)	2.915 (13)	C(2)-N(1)-O(1)	106.7 (7)
P(3)-O(5)-Al(3)	131.1 (3)	N(1)-O(10)	2.964 (8)	C(2)-N(1)-O(10)	115.0 (5)
P(3)-O(6)-Al(1)	143.9 (2)	C(1)-C(3)	1.34 (2)	O(1)-N(1)-O(10)	93.2 (3)
P(1)-O(7)-Al(2)	142.3 (2)	C(2)-C(3)	1.42 (2)	C(1)-C(3)-C(2)	129 (2)
P(1)-O(8)-Al(3)	158.9 (3)	C(3)-C(4)	1.41 (4)	C(1)-C(3)-C(4)	103 (2)
Al(2)-O(9)-Al(3)	144.8 (3)	H(1)-O(9)	0.67 (8)	C(2)-C(3)-C(4)	104 (2)
P(3)-O(10)-Al(3)	139.6 (2)	H(1)-O(5)	2.26 (8)	O(9)-H(1)-O(5)	167 (6)
P(3)-O(11)-Al(2)	137.3 (2)	O(9)-O(5)	2.582 (5)		
P(2)-O(12)-Al(1)	132.0 (2)				
P(2)-O(13)-Al(2)	138.9 (3)				

possible to distinguish clearly between occupancy of a particular site by C and N, and it was not possible to locate any H atoms with certainty. It seems plausible that each molecule of TMPD broke up into one propyl species and two dimethylammonium ions and that the three fragments were encapsulated in the AlPO₄-21 crystals. The refined populations are N(1) 2.84 (7), C(1) 5.70 (13), C(2) 5.18 (9), C(3) 0.88 (8) and C(4) 1.65 (9) atoms/cell; interpretation is uncertain because of overlap (see later). The strongest peak on the final difference synthesis lies at 0.8 Å from O(9), which is undersaturated because of bonding to only two 5-coordinated Al. Although the position is poorly defined, least-squares refinement was successful for a hydrogen atom. The final *R* factor is 0.046, and all deviations from the average structure in $P2_1/a$ must be small.

Description of the Structure

The crystal structure cannot be described adequately by one simple statement, and it is necessary to describe it in several ways using the atomic coordinates (Table II) and interatomic distances (Table III).

Topology of the Aluminophosphate Framework. All three types of P atoms lie at the tetrahedral center of four oxygen atoms, whereas one type of Al atom is in a tetrahedron (Al^{IV}) and the other two types lie in a distorted trigonal bipyramid composed of four oxygen atoms and one hydroxyl molecule (Al^V). Twelve out of the thirteen types of oxygen are bonded to one P and one Al, whereas the thirteenth, O(9), is bonded to two Al^V. Each unit cell contains 4 Al₃P₃O₁₂OH, whose atomic positions can be represented by a 3D net composed of branches linking each oxygen node with two cation nodes. There are four branches to each of the tetrahedral nodes P(1), P(2), P(3), and Al(1) and five branches to the trigonal-bipyramidal nodes Al(2) and Al(3). The 3D net of AlPO₄-21 is unique and novel.

In crystal structures, P typically occurs in a tetrahedron, while Al occurs frequently in a tetrahedron or an octahedron and rarely

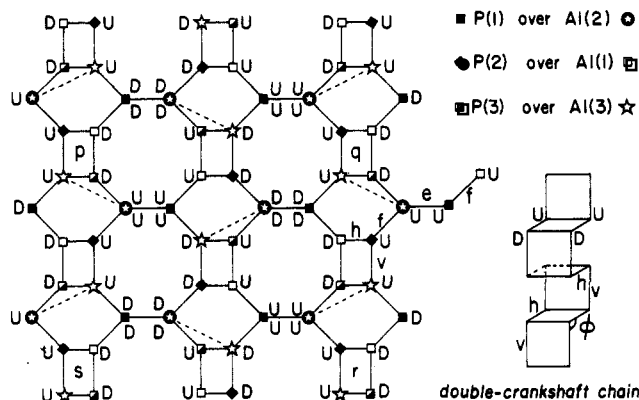


Figure 1. Idealized topologic drawing of the 3D net of $\text{AlPO}_4\text{-21}$. Tetrahedral and trigonal-bipyramidal nodes are represented by square and pentagonal symbols. U and D represent upward- and downward-pointing branches. Each rectangle labeled UDD represents a double-crankshaft chain shown at the right in a contracted position with $\phi = 90^\circ$. The continuous lines would yield a 4-connected 3D net, and the dashed lines convert the Al(2) and Al(3) nodes into 5-connected ones. The unit cell is shown by p, q, r, s. Four types of 4-rings are labeled e, f, h, and v. The axis of projection corresponds to the a axis of the $\text{AlPO}_4\text{-21}$ structure.

in a distorted trigonal bipyramid. Three out of the five published structures with Al^{V} are dense (andalusite,⁷ grandierite,⁸ yoderite⁹), and the distorted trigonal bipyramids share an edge. Augelite¹⁰ contains an $\text{Al}(\text{OH})_4\text{O}_2$ octahedron, an $\text{Al}(\text{OH})_3\text{O}_2$ trigonal bipyramid, and a PO_4 tetrahedron, while senegalite¹¹ has edge and vertex sharing of $\text{Al}(\text{OH})_3(\text{H}_2\text{O})\text{O}_2$ octahedra and $\text{Al}(\text{OH})_3\text{O}_2$ trigonal bipyramids coupled with vertex-sharing of PO_4 tetrahedra to form an open framework. Only octahedra and tetrahedra occur in the $\text{AlPO}_4\text{-15}$ framework,⁴ and the other known frameworks of aluminum phosphates contain alternating AlO_4 and PO_4 tetrahedra.^{1-3,14}

Because each oxygen and hydroxyl of the $\text{AlPO}_4\text{-21}$ framework is 2-connected, it is convenient to consider just the branches between adjacent Al and P. Consider a 3-connected 2D net composed of quadrilaterals, hexagons, and octagons (Figure 1). Regularity is not possible for both the hexagons and octagons. In the most regular shape, there are two types of nodes with circuit symbols 4.6.8 and 6.8.8. This 2D net can be converted into a 4-connected 3D net by addition of a branch to each node. Enumeration of the infinity of possible 3D nets is described elsewhere. As in Figure 1v of ref 12, the sequence up-up-down-down for addition of a vertical branch to each node of a horizontal 4-ring (h) produces a double-crankshaft chain (Figure 1, lower right), represented by UDD. The particular arrangement of double-crankshaft chains in Figure 1 is characterized by a UUUUUDDD sequence around each 8-ring and a UUUUUDDD sequence around each 6-ring. To obtain the net for $\text{AlPO}_4\text{-21}$, convert each 6-ring into a 3-ring and a 5-ring by addition of a branch shown by a dashed line. The nodes marked by a pentagonal symbol become 5-connected, whereas those marked by a square remain 4-connected.

Considerable distortion occurs from the idealized geometry in Figure 1. Each crankshaft flexes as the angle ϕ increases from 90° to about 140° , and the a repeat of 10.33 Å in $\text{AlPO}_4\text{-21}$ is much longer than the 8.45-Å repeat in feldspars.¹³ In Figure 1, the ideal square of the 2D net is replaced by a rectangle with an edge ratio near 0.7. Furthermore, the ideal 2D net becomes corrugated so that the 3- and 5-rings can become more regular, and the

crankshafts also become twisted. Finally, the alternation of Al and P around the 4-, 6-, and 8-rings produces a minor perturbation. Each vertical branch in Figure 1 connects P(3) to Al(3), or P(1) to Al(2), or P(2) to Al(1).

The stereoplot of Figure 2 is arranged with the b axis upward and the a and c axes to the left and right, respectively, of the bottom center. Two double-crankshaft chains lie parallel to a at about one-fourth and three-fourths of b . The extension and twisting of each chain are obvious. Each 5-coordinated Al is shown by an open circle, and each 4-coordinated Al by a dot. Some readers may find it helpful to color the two types of 4-rings in the crankshaft chains: each type obeys the symmetry of the a -glide planes at $y = 1/4$ or $3/4$. A third type of 4-ring is shaped like a rhombus and occurs at each corner of the unit cell and at the face center $1/2, 1/2, 0$. This began as a branch (labeled e) between adjacent octagons in the 2D net of Figure 1 and turned into the DD or UU bridge of the 3D net ($\text{Al}(2)\text{P}(1)\text{Al}(2)\text{P}(1)$). This e-bridge lies between two 5-rings, two 3-rings, and two 4-rings of yet another type which began as a branch between an octagon and a hexagon (f, Figure 1). The f-bridge joins the double-crankshaft chain with the e-bridge. Each e-bridge lies at a center of symmetry and joins with two f-rings and two v-rings to form a fragment of five edge-shared 4-rings (UUUUU or DDDDD, Figure 1); only four out of five rings are shown in Figure 2.

Each 3-ring from Figure 1 is easily recognized in Figure 2, but note that the fifth branch is not drawn for some of the 5-connected nodes (open circle). However, it is easy to misidentify the 5-ring from Figure 1 because there are two different types. The horizontal 5-ring from Figure 1 is represented by a chair-shaped 5-ring in Figure 2, one of whose edges is attached to a crankshaft chain. A second type of 5-ring is nearly planar, and it shares edges with two 3-rings and one 4-ring of type 3. It is superimposed on a 3-ring in Figure 1; whereas a 3-ring is simply given by horizontal branches between UUD, a 5-ring is obtained by using additional vertical branches at each U. Indeed, alternate 3- and 5-rings generate a chain parallel to the a axis, which shares edges with a double-crankshaft chain.

Figure 3 shows the linkages between the chains. In the left-hand drawing, the nodes of the two double-crankshaft chains are coded for the chemical type and labeled d-i and p-w. In the right-hand drawing, the 3- and 5-rings of the chains are cross-linked with the rhombus-shaped 4-rings to form a complex 2D net at each ab face of the unit cell. Chains of nodes d-i and p-w can be matched with those in the left-hand drawing.

The framework contains a 3D pore system defined by 8-rings. A channel along the a axis is bounded in the b direction by the double-crankshaft chains (Figure 2), and the cross section is idealized as an UUUUUDDD octagon in Figure 1. Adjacent channels in the c direction are connected by chair-shaped octagons suspended between 3-, 4-, and 5-rings (Figure 2, ab face of unit cell; Figure 3). Each channel has boat-shaped side pockets, each comprised of a boat-shaped 8-ring, two chair-shaped 5-rings, a planar 5-ring, a 3-ring, and an f-type 4-ring.

The $\text{AlPO}_4\text{-21}$ net has a greater density of branches in corrugated sheets lying near $y = 1/4$ and $3/4$. These sheets are bridged by e-type 4-rings.

Geometry of the Aluminophosphate Framework. Figure 4 is a b -axis projection of all the atoms in the 3D net. A double-crankshaft chain is shown by dots, four 3-rings by heavy lines, and six 4-rings of type e by dashes. Figure 5 is a stereoplot showing branches to all the oxygen species of the framework.

The PO_4 groups have close to ideal tetrahedral geometry with P-O distances ranging only from 1.509 to 1.542 Å and O-P-O angles from 106.3 to 112.1° (Table III). The Al(1) tetrahedron is also nearly regular: Al-O = 1.718–1.751 Å; O-Al-O = 107.2 – 112.8° . These distances are close to those for other aluminophosphate frameworks: e.g. 1.510–1.546 Å in $\text{AlPO}_4\text{-15}$,⁴ 1.514–1.546 Å in senegalite,¹¹ and 1.516 and 1.739 Å in berlinite.¹⁴

The Al(2) and Al(3) polyhedra show some distortion from an Archimedean trigonal bipyramid. Oxygen of type 9 is shared between these polyhedra and is bonded to a hydrogen atom to form a hydroxyl group. Although the accuracy of the hydrogen position

(7) Burnham, C. W.; Buerger, M. J. *Z. Kristallogr.* **1961**, *115*, 269–290.

(8) Stephenson, D. A.; Moore, P. B. *Acta Crystallogr., Sect. B* **1968**, *B24*, 1518–1522.

(9) Fleet, S. G.; Megaw, H. D. *Acta Crystallogr.* **1962**, *15*, 721–724.

(10) Araki, T.; Finney, J. J.; Zolnai, T. *Am. Mineral.* **1968**, *53*, 1096–1103.

(11) Keegan, T. D.; Araki, T.; Moore, P. B. *Am. Mineral.* **1979**, *64*, 1243–1247.

(12) Smith, J. V. *Am. Mineral.* **1978**, *63*, 960–969.

(13) Smith, J. V. "Feldspar Minerals"; Springer Verlag: Heidelberg, 1975.

(14) Schwarzenbach, D. *Z. Kristallogr.* **1966**, *123*, 161–185.

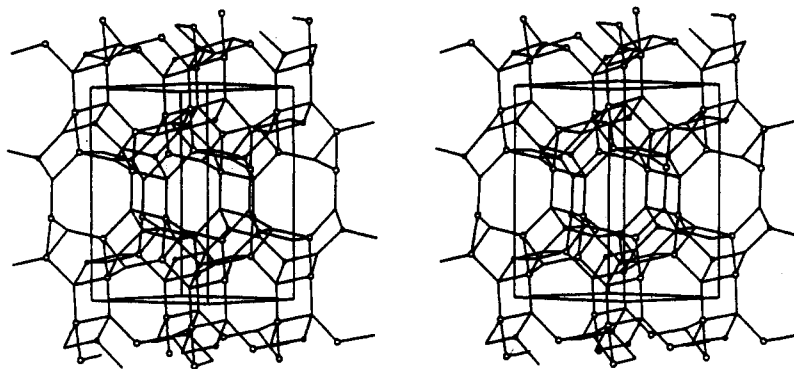


Figure 2. Stereoplots of the framework of the $\text{AlPO}_4\text{-21}$ structure. Each line represents a branch connecting two nodes occupied by tetrahedral Al (dot), trigonal-bipyramidal Al (circle), or tetrahedral P (unmarked). An oxygen atom would lie near the center of each branch. The unit cell has b upward, a leftward, and c backward to the right from the front right-hand corner. Some nodes at the edge of the net lack a branch.

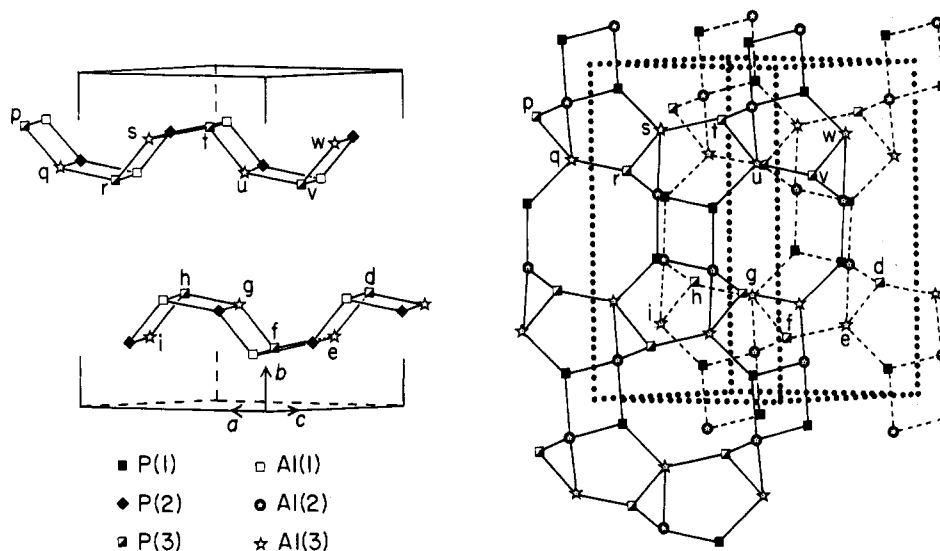


Figure 3. Tessellations and chains in the $\text{AlPO}_4\text{-21}$ structure. The unit cell is rotated about 30° with respect to that in Figure 2, as may be seen by matching the double-crankshaft chains in the left-hand drawing. In the right-hand drawing, a nonplanar tessellation of triangles, squares, pentagons, and octagons (continuous line) lies near the front ab face of the unit cell, and an identical one (dashed line) lies near the back face. Nodes marked d - i and p - w are shared with double-crankshaft chains.

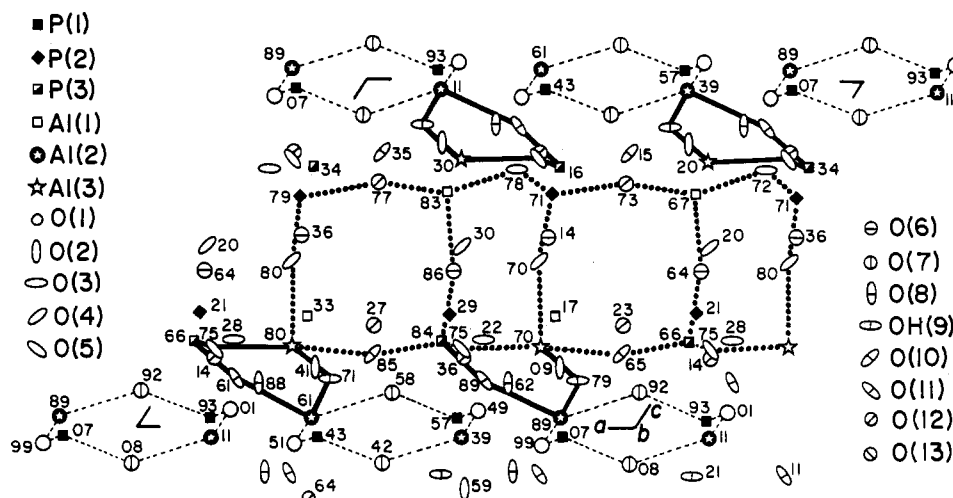


Figure 4. Projection of all the framework atoms down the b axis. Some 3- and 4-rings are outlined. Height is in hundredths of b .

is low, it appears that it is hydrogen bonded across a 5-ring to O(5). The Al-OH distances of 1.830 and 1.936 Å fall within the wide ranges of 1.816–1.935 Å for senegalite¹¹ and 1.864–1.983 Å for augelite,¹⁰ and the Al-O distances of 1.779–1.889 Å (mean 1.820 Å) can be matched with Al-O distances of senegalite¹¹ (1.788–1.870 Å; mean 1.835 Å). O(9) is a trigonal apex in the Al(2) polyhedron, and the O(1)-Al(2)-O(9) angle of 173.5° is close to the ideal value of 180° . The other angles of 86.3 – 97.0

and 112.1 – 133.6° deviate modestly from the ideal 90 and 120° . In the Al(3) polyhedron, O(9) is not a trigonal apex, and the corresponding values are 173.6, 86.0–93.4, and 109.1 – 134.5° .

In the PO_4 tetrahedra, the four oxygens shared with tetrahedral Al are longer (1.530–1.542 Å; mean 1.538 Å) than the eight oxygens bonded with trigonal-bipyramidal Al (1.509–1.525 Å; mean 1.520 Å), in accordance with bonding theory (e.g., see ref 15). In the $\text{AlO}_4(\text{OH})$ trigonal bipyramid, the apical oxygens

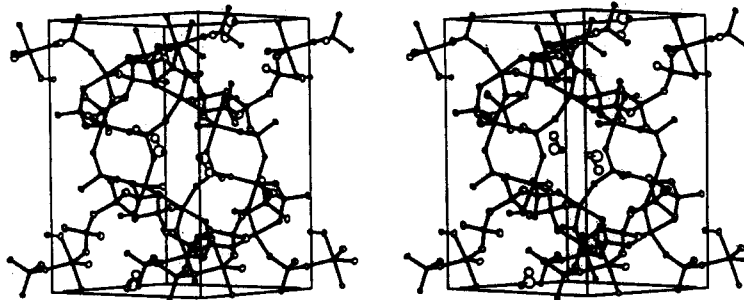


Figure 5. Stereplot of all atoms in the $\text{AlPO}_4\text{-21}$ framework together with the C(1)–N(1)–C(2) positions assigned to dimethylammonium ions. Compare with Figure 2.

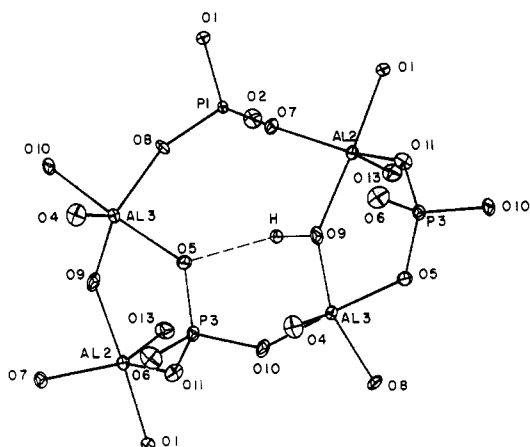


Figure 6. Environment of the hydroxyl group, showing hydrogen bonding across a 5-ring. See Figure 5 for a stereplot of atomic positions.

are more distant than the ones in the waist, and the hydroxyls are more distant than the oxide ions for a chosen position: apical hydroxyl, 1.936 Å; apical oxide, 1.864, 1.867, 1.889 Å; waist hydroxyl, 1.830 Å; waist oxide, 1.779–1.796 Å. The most distant apices O(1) at 1.867 Å and O(10) at 1.889 Å are 2.92 and 2.96 Å, respectively, from N(1), the position believed to be occupied mainly by the nitrogen atom of a dimethylammonium ion (next section). This is consistent with weakening of the Al–O bond by hydrogen bonding to the nitrogen. Hybridization of the sp^2 orbitals of Al can explain the apical elongation of the trigonal bipyramids.¹⁶ Thus all the distances in the polyhedra are explained by simple theory involving only first and second neighbors.

Position of the Hydrogen Atom in the Hydroxyl Group. Figure 6 shows how the hydrogen atom occupies a position that maximizes its distance from Al(2) and Al(3) and allows hydrogen bonding to O(5) across the 5-ring. This hydrogen bonding is important for determining the topology and geometry of the framework. Removal of each hydroxyl group O(9)–H(1) would allow Al(2) and Al(3) to become tetrahedrally coordinated, as each pair of adjacent 3- and 5-rings turns into a 6-ring. The resulting framework would have orthorhombic topological symmetry (Figure 1). Indeed $\text{AlPO}_4\text{-21}$ transforms into $\text{AlPO}_4\text{-25}$ upon calcination, and the new powder pattern has only half the number of lines. X-ray data are being collected for $\text{AlPO}_4\text{-25}$ to determine whether the undashed lines in Figure 1 represent its framework topology.

Channel Contents. As described in the Experimental Section, each unit cell should contain 1.33 $\text{N}_2\text{C}_7\text{H}_{21}$. There are three strong and two weak electron density peaks. The three strongest peaks N(1), C(1), and C(2) are tentatively assigned to a dimethylammonium species, which could be derived from the trial template TMPD by fission. The two weakest peaks C(3) and C(4) together with part of the C(1) or C(2) peak are assigned to a three-carbon species. Quantitative fission of the template would provide twice

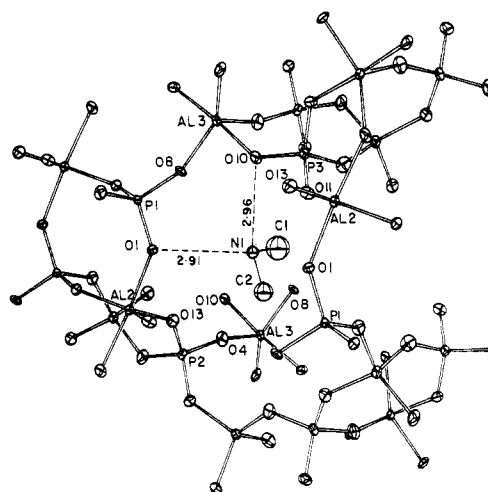


Figure 7. Environment of N(1), C(1), and C(2). See Figure 5 for a stereplot of atomic positions.

as many dimethylammonium species as propyl species, but it is impossible to obtain a reliable interpretation of the electron density peaks because of overlap and incomplete refinement of H atoms. Within experimental error, complete disorder would be allowed between the two chemical species. However, assignment of most of the N(1) electron density to a nitrogen atom is likely because this would allow hydrogen bonding to O(1) and O(10) at 2.91 and 2.96 Å (Figure 7). All the C sites are far enough from framework oxygens to be consistent with van der Waals bonding (over 2.9 Å).

General Remarks

The unique and novel framework of $\text{AlPO}_4\text{-21}$ has several important features: (a) a 3-ring composed of two 5-coordinated Al atoms and one tetrahedrally coordinated P atom, (b) two types of 5-rings containing two and three Al^{V} atoms, respectively, (c) four types of 4-rings, two of which combine into an extended double-crankshaft chain, (d) a chain of edge-sharing 3- and 5-rings, and (e) a tessellation composed of 3-, 4-, 5-, and 8-rings. The pairs of adjacent Al^{V} atoms share a hydroxyl group, whose removal during calcination might yield a new net containing 4-, 6-, and 8-rings. Because Al is now demonstrated to occur in 4-, 5-, and 6-coordination in frameworks, the chemistry of the aluminophosphates may turn out to be more complex than for the aluminosilicates, where Al has been found only in 4-coordination so far.

Apart from the sharing of a hydroxyl group by adjacent Al^{V} atoms, all oxygen atoms are linked to one Al and one P atom as expected for a simple ionic model. Hydrogen bonding across a 5-ring is probably important for structural stability. All interatomic distances are consistent with simple chemical models involving near neighbors. Particularly interesting is the greater displacement of oxygen atoms at the trigonal apices of the trigonal bipyramids than the oxygen atoms at the waist; this can be explained by a molecular-orbital effect.

Although the contents of the channel system could not be specified precisely, the bulk chemical composition and the electron

(15) Brown, I. D.; Shannon, R. D. *Acta Crystallogr., Sect. A* **1973**, *A27*, 266–282.

(16) Hill, R. J.; Gibbs, G. V.; Peterson, R. C. *Aust. J. Chem.* **1979**, *32*, 231–241.

density peaks imply that each TMPD molecule used as an attempted template had been fissioned into three triatomic species during incorporation into the $\text{AlPO}_4\cdot 21$ structure. These species probably consist of two dimethylammonium and one propyl species. For each unit cell, the $\text{Al}_{12}\text{P}_{12}\text{O}_{48}(\text{OH})_4$ framework lacks four positive charges, which could be balanced by some combination of the four dimethylammonium and propyl species; both charged and uncharged species are needed. Nuclear magnetic resonance spectroscopy should provide an accurate identification. Although the occluded species fit neatly into the channels, the occurrence of two orientations of the triatomic species suggests that any templating control is weak at best. The doubling of high-angle diffractions might result from small changes of cell dimension induced by the different orientations; if so, each single crystal is actually an aggregate of two types of crystallites in near-parallel orientation. Electron microscopy and energy loss

spectroscopy might provide a test of this idea.

The subunits of the framework of $\text{AlPO}_4\cdot 21$ can be arranged in many different ways, and systematic enumeration is in progress. The twinning of $\text{AlPO}_4\cdot 21$ crystals is explained by a simple stacking fault.

Acknowledgment. The contribution by G.A., J.J.P., and J.V.S. was supported primarily by National Science Foundation Grant CHE 80-24138 and secondarily by the Materials Research Laboratory funded by NSF Grant 79-24007. We thank N. Weber for technical help and E. M. Flanigen, S. T. Wilson, and L. Patton for assistance and discussion.

Supplementary Material Available: Listings of observed and calculated structure factors (Table IV) and anisotropic displacement factors (Table V) (13 pages). Ordering information is given on any current masthead page.

Contribution from the Department of Chemistry,
University of Massachusetts, Amherst, Massachusetts 01003

Stereochemically Nonrigid Five-Coordinated Germanates. Synthesis and Structure of Hydroxy- and Halo-Containing Spirocyclic Germanium(IV) Complexes^{1,2}

ROBERT R. HOLMES,* ROBERTA O. DAY, ARJUN C. SAU, CHARLES A. POUTASSE,³
and JOAN M. HOLMES

Received May 30, 1984

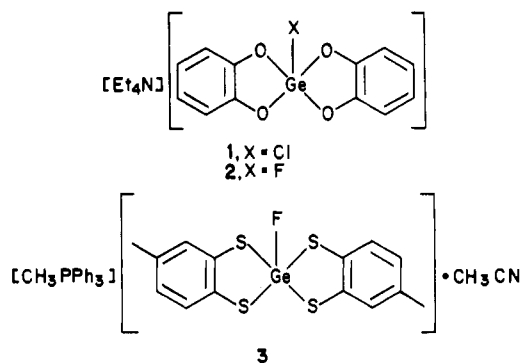
A series of five-coordinated anionic germanates containing oxygen and sulfur ligands, $[\text{Et}_4\text{N}][(\text{C}_6\text{H}_4\text{OS})_2\text{GeX}]$ ($\text{X} = \text{F}, \text{Cl}, \text{Br}, \text{I}$), were synthesized from the newly formed spirocyclic compound $(\text{C}_6\text{H}_4\text{OS})_2\text{Ge}$ and Et_4NX . Also formed was the hydroxy derivative $[\text{Et}_3\text{NH}][(\text{C}_6\text{H}_4\text{OS})_2\text{GeOH}]$. The X-ray structures of chloro and bromo derivatives, **4** and **5**, respectively, were obtained as well as the structures of the previously prepared bromo and hydroxy catecholates, $[\text{Et}_4\text{N}][(\text{C}_6\text{H}_4\text{O}_2)_2\text{GeBr}]$ (**6**) and $[\text{Et}_3\text{NH}][(\text{dtbc})_2\text{GeOH}]$ (**7**) (dtbc is 3,5-di-*tert*-butylcatechol). These compounds form a series, showing distortions from the trigonal bipyramid to the rectangular pyramid: **4** (34.2%); **5** (23.6, 26.2%); **6** (70.4%); **7** (95.7%). As with phosphoranes, the dominant criterion to stabilize the square or rectangular pyramid for pentacoordinate germanium is the presence of two unsaturated five-membered rings with like atoms in any one ring directly attached to the central atom. Comparisons with related silicon and tin anionic five-coordinated complexes suggest that stereochemical nonrigidity increases from silicon to germanium to tin. **4** crystallizes in the monoclinic space group *Cc* with $a = 10.869$ (3) Å, $b = 12.852$ (4) Å, $c = 16.798$ (4) Å, $\beta = 103.00$ (2)°, and $Z = 4$. **5** crystallizes in the monoclinic space group *P2*₁ with $a = 12.345$ (2) Å, $b = 27.800$ (5) Å, $c = 7.779$ (1) Å, $\beta = 104.54$ (1)°, and $Z = 4$. **6** crystallizes in the monoclinic space group *P2*₁/*c* with $a = 11.144$ (1) Å, $b = 10.916$ (2) Å, $c = 18.293$ (2) Å, $\beta = 96.89$ (1)°, and $Z = 4$. **7** crystallizes in the orthorhombic space group *Pna2*₁ with $a = 21.415$ (5) Å, $b = 16.279$ (5) Å, $c = 10.297$ (3) Å, and $Z = 4$. The final conventional unweighted residuals were 0.037 (**4**), 0.051 (**5**), 0.059 (**6**), and 0.061 (**7**).

Introduction

Recent work^{4,5} on five-coordinated compounds of main-group 4 elements has concentrated on anionic derivatives of silicon(IV) containing a spirocyclic framework. From the X-ray structural investigations, a distortion coordinate resulted⁴ that was closely analogous to the Berry coordinate that was found earlier for phosphoranes.^{6,7} This work resulted in the formulation of structural principles for five-coordinated silicon⁵ that were comparable to those that apply to isoelectronic pentacoordinated phosphorus compounds.⁶⁻⁹

In an extension to related germanium complexes, the only examples that have been structurally characterized are the bis-

(benzenediolato)chlorogermanates¹⁰ and -fluorogermanates,¹¹ **1** and **2**, respectively, and the corresponding bis(dithiolato)fluorogermanate¹¹ (**3**).



- (1) Pentacoordinated Molecules. 58. Previous paper in the series: Vollano, J. F.; Day, R. O.; Rau, D. N.; Chandrasekhar, V.; Holmes, R. R. *Inorg. Chem.* **1984**, *23*, 3153.
- (2) Presented in part at the Fourth International Conference on the Organometallic and Coordination Chemistry of Germanium, Tin, and Lead, Montreal, Quebec, Aug 1983; Abstr. F-4, p 33.
- (3) This work represents in part a portion of: Poutasse, Charles A., III. Ph.D. Thesis, University of Massachusetts, Amherst, MA, 1983.
- (4) Holmes, R. R.; Day, R. O.; Harland, J. J.; Sau, A. C.; Holmes, J. M. *Organometallics* **1984**, *3*, 341.
- (5) Holmes, R. R.; Day, R. O.; Harland, J. J.; Holmes, J. M. *Organometallics* **1984**, *3*, 347.
- (6) Holmes, R. R.; Deiters, J. A. *J. Am. Chem. Soc.* **1977**, *99*, 3318.
- (7) Holmes, R. R. *Acc. Chem. Res.* **1979**, *12*, 257.
- (8) Holmes, R. R. *ACS Monogr.* **1980**, No. 176, Chapter 2.
- (9) Holmes, R. R. *J. Am. Chem. Soc.* **1978**, *100*, 433.

- (10) Sau, A. C.; Day, R. O.; Holmes, R. R. *J. Am. Chem. Soc.* **1980**, *102*, 7972.
- (11) Day, R. O.; Holmes, J. M.; Sau, A. C.; Holmes, R. R. *Inorg. Chem.* **1982**, *21*, 281.